Published in final edited form as:
J Phys Chem Lett. ; 3(16): 2293–2297. doi:10.1021/jz300768g.

Weakly Antiferromagentic Coupling Via Superexchange Interaction Between Mn(II)-Mn(II) Atoms: A QM/MM Study of the Active Site of Human Cytosolic X-Propyl Aminopeptidase P

Sangwook Wu[1], **Shubin Liu**[2], **Sooyeon Sim**[1], and **Lee G. Pedersen**[1]

Shubin Liu: shubin@email.unc.edu; Lee G. Pedersen: lee_pedersen@unc.edu

[1]Department of Chemistry, University of North Carolina, Chapel Hill, North Carolina 27599-329

[2]Research Computing Center, University of North Carolina, Chapel Hill, North Carolina 27599-3420

Abstract

We investigate the dinuclear manganese, Mn(II)-Mn(II), active site of human cytosolic X-propyl aminopeptidase (XPNPEP1) employing the QM/MM method. The optimized structure supports two manganese atoms at the active site and excludes the possibility of a single Mn(II) atom or other combination of divalent metal ions: Ca(II), Fe(II), Mg(II). A broken symmetry solution verifies an antiferromagnetically coupled state between the Mn(II)-Mn(II) pair, which is the ground state. From the energy difference between the high spin state (HS) and the broken symmetry state (BS), we estimate the exchange coupling constant, J, to be 5.15 cm^{-1}. Also, we observe multiple bridges (p orbitals) from solvent and two carboxylate linking to the Mn(II)-Mn(II), which leads to the weakly antiferromagnetic interaction of d^5-d^5 electrons through superexchange coupling.

Keywords

Dinuclear Manganese Atoms; Broken Symmetry; Enzyme; EPR; μ-carboxylato bridge; μ-H_2O bridge

---

Human cytosolic X-propyl aminopeptidase (XPNPEP1) degrades a blood pressure-controlling peptide, bradykinin (a 9 amino acid chain)[1]. It's action leads to lowering blood pressure by cleaving an Arg-Pro bond[2]. Recently, the structure of 70-kDa cytosolic XPNPEP1 with three distinct domains was crystallized[3]. The X-ray crystal structure reveals that XPNPEP1 employs two divalent manganese atoms (Mn(II)-Mn(II)) in the active site. In the crystallization process of XPNPEP1, the molar ratio between manganese and protein in manganese-rich LB (Luria-Bertani) media is 1.79:1, implying the XPNPEP1 employs two manganese Mn(II)-Mn(II) for the catalytic activity[3]. However, in a different plain LB media, the molar ratio between manganese and protein is 0.69:1. This indicates that the XPNPEP1 requires only a single manganese atom[3]. In addition, the data in plain LB media shows that the molar ratio between Mg(II)/protein, Ca(II)/protein, and Fe(II)/protein is 0.49:1, 0.02:1, and 0.73:1, respectively. This data suggests a possible combination of a single Mn(II) with an other divalent metal ion. In this work, we report a computational study of the Mn(II)-Mn(II) active site by employing QM/MM approach (Figure 1).

Correspondence to: Shubin Liu, shubin@email.unc.edu; Lee G. Pedersen, lee_pedersen@unc.edu.

The authors declare no competing financial interest.

We examine the possibility of the combination of Mn (II) with other divalent metal ions. Several specific residues around the active site are prepared for the QM/MM calculation using the X-ray crystal structure (PDB code : 3CTZ)[3]. D415, D426, E523, E537, H489, H498, and six X-ray resolved water molecules (denoted as W1-W6 in Figure 1) and two Mn(II) atoms are treated as the QM region. On the other hand, F381, V427, S416, T428, T425, and R535 are treated as MM region. A charge embedding method was employed[4]. C_β and C_γ carbons for D415 and D426 are included in QM region. Likewise, C_δ and C_γ carbons for E523 and E537 are included in the QM region. Finally, for H498 and H498, the imidazole ring is included in the QM region. The link atom model is used for the atoms in the QM and MM interface. The ligand, hexaethylene glycol in the X-ray crystal structure, is included in our QM/MM simulation. For histidine, the δ nitrogen of the imidazole ring is protonated to ensure neutral conditions. The model is energy optimized using ONIOM[5,6] approach in the Gaussian09 package. The universal force field (UFF)[7] was employed for the molecular mechanics calculation and density functional theory[8] with the B3LYP exchange-correlation functional used in the QM region[9]. A mixed basis set was utilized with N and O elements defined by a 6-311+G(d) basis set, metal ions using the 6-311G(d) basis set and C and H elements using 6-31G(d) basis set. The Mn(II)-Mn(II) atoms generate multiple spin states from high spin (HS) (S=5) to low spin (LS) (S=0). We find trigonal-bipyramidal geometry for the coordination of Mn1: D415 (Oδ-1), D426 (Oδ-1), E537 (Oε-1), W1 (O), and W2 (O) from the Mn1[3]. Similarly, we find a distorted octahedral geometry for the coordination of Mn2: D426 (Oδ-2), E523 (Oε-2), E537 (Oε-2), H489 (Nε-2), W1, and W3[3] (Table 1). An asymmetric coordination geometry for both manganese atom is also reported in the liver arginase structure (PDB code : 1RLA)[10]. The distance between the Mn(II)-Mn(II) atoms in the optimized structure for the HS state (S=5) is 3.47 Å, which shows quite consistent with the Mn(II)-Mn(II) distance measured in the X-ray structure, 3.42 Å. In addition, the other coordination values of two Mn(II)-Mn(II) atoms with neighboring key residues for the HS state (S=5) show also quite consistent with the X-ray structure (Table 1). On the other hand, the distance between the Mn(II)-Mn(II) atoms for the closed shell LS state (S=0) is much shorter than the X-ray value (2.76 Å).

Other discrepancies are also observed: the distance for W1-Mn1 and W1-Mn2 are 1.88 Å (2.23 Å in X-ray structure) and 1.95 Å (2.31 Å in X-ray structure). Likewise, the side chain conformations of two residues, H498 and H489, are severely distorted in the closed shell LS state (S=0). We investigated the coordination geometry when one of Mn(II) atoms, Mn1, is substituted by the other divalent metal ions: Ca(II), Mg(II) and Fe(II). After the substitution, we observe significant modification for the positions of the water molecule (W1) is shifted toward the substituted metal ions (Ca, Fe, and Mg), leading to a distortion of the geometry coordination with Mn2. The positions of the water molecules (W2 and W3) are well conserved for the metal ion substitution at the site 1 while the water position of the water molecule (W1) (Table 1). With an exception of Mg-Mn (S=1/2), the molecules (W1) are not conserved and instead are repelled from the active site. (Figure 2)

Subsequently, we performed geometrically optimization for single Mn(II) at the site 2 (no metal ion at the site 1). The geometrically optimized structure for the single Mn(II) is shown (Figure 3). The water molecule (W2) occupies the vacant site of the metal ion at the site 1.

However, we observe a severe distortion residue E537. The energy calculation employing ONIOM [5,6] model estimates that the HS state (S=5) is lower in energy than the closed-shell LS state (S=0) by +146.89 kcal/mol. However, the broken symmetry (BS) state[12] employing the geometrically optimized structure is estimated to be lower than the HS state (S=5) by −0.37 kcal/mol. The estimation suggests that the antiferromagetic BS/LS state (S=0) is a ground state. This calculation is performed by the ORCA program[14,15] with the hybrid of

spin-unrestricted Hartree-Fock (UHF) with B3LYP DFT method[9]. The dinuclear manganese atoms, Mn(II)-Mn(II), in the active site are described by the Heisenberg spin Hamiltonian,

$$H = -2J\mathbf{S}_1 \cdot \mathbf{S}_2 \quad (1)$$

In the spin Hamiltonian, $\mathbf{S_1}$ and $\mathbf{S_2}$ are spin vector operators of the Mn(II) atoms at the site 1 and site 2, respectively. J is exchange coupling constant between the two Mn(II) atoms, indicating that J > 0 in the ferromagnetic state while J < 0 antiferromagnetic state. The energy difference between the HS and BS provides a clue to estimate the exchange coupling constant J from the relation of [16,17]

$$J = -(E_{HS} - E_{BS})/(\langle S^2_{HS}\rangle - \langle S^2_{BS}\rangle), \quad (2)$$

where **S** is the total spin operator, $\mathbf{S}=\mathbf{S}_1+\mathbf{S}_2$. And E_{HS} and E_{BS} are the energies for the HS and BS state. The expectation value of the square of the total spin operator, $< S^2 >$ is given as [18,19]

$$\langle S^2\rangle = \left(\frac{N^\alpha - N^\beta}{2}\right)\left(\frac{N^\alpha - N^\beta}{2}+1\right) + N^\beta - \sum_i f_i^\alpha f_i^\beta \left|S_{ij}^{\alpha\beta}\right|^2 \quad (3)$$

where *N, N* are number of spin-up and spin-down electrons. N^α =152 and N^β =152. f_i^α and f_i^β are the spin-orbital occupation number (0 or 1). And $S^{\alpha\beta}{}_{ii}$ is a spatial orbital overlap integral[20]. From the above relation, we estimate the exchange coupling constant as J=−5.15 cm^{-1}, indicating that the Mn(II)-Mn(II) atoms in the active site are weakly antiferromagnetically coupled. The energy differences for similar systems have been shown to be not strongly dependent on which hybrid functional is used[21,22].

The J value for the human cytosolic X-propyl aminopeptidase (XPNPEP1) has not been reported so far, however, the electron paramagnetic resonance (EPR) experiment for the aminopeptidase P (AMPP; EC 3.4.11.9; PepP protein) from *E. coli* reveals the exchange coupling constant, J, is antiferromagnetic with $|J| \gg 2.0\ cm^{-1}$ [23]. The schematic superexchange interaction[24] as shown in Figure 4 is mediated via orbital mixing from water molecule (W1) with the bridges: (μ-H_2O), bis (μ-carboxylato). Subsequently, the two highest overlaps between two magnetic molecular orbitals among the d^5 unpaired electrons at the manganese atoms are shown. (Figure 5): two dominant superexchange pathways.

For the 148th electrons, the d_z^2 spatial orbital overlaps with the d_{yz} spatial orbital with $S^{\alpha\beta}$=0.063 via μ-carboxylato and μ-H_2O bridges. On the other hand, for the 149th electrons, a spin in the d_{xz} spatial orbital overlaps with the d_{xy} spatial orbital with $S^{a\beta}$=0.031 via μ-carboxylato and μ-H_2O bridges. Experimental EPR values of exchange coupling constants for the dinuclear manganese clusters with mixed (μ-H_2O) bis(μ-carboxylato) bridges and dinuclear manganese enzymes are listed (Table 2). Dinuclear manganese (II) clusters belonging to this class exhibit weakly antiferromagnetic states.

Qualitatively, the addition of μ-carboxylato bridges increase the distance between the Mn(II)-Mn(II) atoms[27], which decreases J exponentially. The electron density of water molecule (W1) is low as shown in Figure 5. The electron density of two carboxylates from D426 and E537 is high, however, the relative angles of the oxygens is not effective for superexchange pathways (angle Mn1- Oδ1(D426)-Mn2 ~ 70°). These lead to a relatively smaller spatial overlaps and but still (apparently) facilitate weak antiferromagnetic coupling between the manganese atoms at the active site. As the role of this antiferromagnetic effect in catalysis is unknown, we shall look forward to future work that clarifies this phenomena in a biological context.

Acknowledgments

SBL was supported as part of the UNC EFRC: Solar Fuels, an Energy Frontier Research Center funded by the U.S. Department of Energy, Office of Science, and Office of Basic Energy Sciences under Award No. DE-SC0001011. LGP acknowledges NIH grant HL-06350 and NSF FRG DMR 084549.

References

1. Prechel MM, Orawski AT, Maggiora LL, Simmons WH. Effect of a New Aminopeptidase P Inhibitor, Apstatin, on Bradykinin Degradation in the Rat Lung. J Pharmacol Expt Therap. 1995; 275:1136–1142.
2. Simmons WH, Orawski AT. Membrane-Bound Aminopeptidase-P from Bovine Lung - Its Purification, Properties, and Degradation of Bradykinin. J Biol Chem. 1992; 267:4897–4903. [PubMed: 1537867]
3. Li X, Lou Z, Li X, Zhou W, Ma M, Cao Y, Geng Y, Bartlam M, Zhang XC, Rao Z. Structure of Human Cytosolic X-prolyl Aminopeptidase - A Double Mn(II)-Dependent Dimeric Enzyme with a Novel Three-domain Subunit. J Bio Chem. 2008; 283:22858–22866. [PubMed: 18515364]
4. Mayhall NJ, Raghavhacari K, Hratchian HT. ONIOM-Based QM:QM Electronic Embedding Method Using Lowdin Atomic Charges: Energies and Analytic Gradients. J Chem Phys. 2010; 132:114107. [PubMed: 20331281]
5. Vreven T, Morokuma K, Farkas O, Schlegel HB, Frisch MJ. Geometry Optimization with QM/MM, ONIOM, and Other Combined Methods. I. Microiterations and Constraints. J Comput Chem. 2003; 24:760–769. [PubMed: 12666168]
6. Dapprich S, Komaromi I, Byun KS, Morokuma K, Frisch MJ. A New ONIOM Implementation in Gaussian98. Part I. The Calculation of Energies, Gradients, Vibrational Frequencies and Electric Field Derivatives. J Mol Struct. 1999; 462:1–21.
7. Rappe AK, Casewit CJ, Colwell KS, Goddard WA III, Skiff WM. Uff, a Full Periodic-Table Force-Field for Molecular Mechanics and Molecular-Dynamics Simulations. J Am Chem Soc. 1992; 114:10024–10035.
8. Parr, RG.; Yang, Y. Density-Functional Theory of Atoms and Molecules. Oxford University Press; Oxford: 1989.
9. Stephens PJ, Devlin FJ, Chabalowski CF, Frisch MJ. Ab-Initio Calculation of Vibrational Absorption and Circular-Dichroism Spectra Using Density-Functional Force-Fields. J Phys Chem. 1994; 98:11623–11627.
10. Kanyo ZF, Scolnick LR, Ash DE, Christianson DE. Structure of a Unique Binuclear Manganese Cluster in Arginase. Nature. 1996; 383:554–557. [PubMed: 8849731]
11. Suzuki, M.; Suzuki, IS. [October 7, 2011] Lecture Notes on Solid State Physics (superechange interaction). www2.binghamton.edu/physics/docs/super-exchange.pdf
12. Noodleman L. Valence Bond Description of Anti-Ferromagnetic Coupling in Transition-Metal Dimers. J Chem Phys. 1981; 74:5737–5743.
13. Noodleman L, Davidson ER. Ligand Spin Polarization and Antiferromagnetic Coupling in Transition-Metal Dimers. Chem Phys. 1986; 109:131–143.
14. Neese F. Prediction of Electron Paramagnetic Resonance g Values Using Coupled Perturbed Hartree-Fock and Kohn-Sham Theory. Chem Phys. 2001; 115:11080–11096.
15. Neese F. Definition of Corresponding Orbitals and the Diradical Character in Broken Symmetry DFT Calculations on Spin Coupled Systems. J Phys Chem Solid. 2004; 65:781–785.
16. Soda T, Kitagawa Y, Onishi T, Takano Y, Shigeta Y, Nagao H, Yoshioka Y, Yamaguchi K. Ab Initio Computations of Effective Exchange Integrals for H-H, H-He-H and Mn_2O_2 Complex: Comparison of Broken-Symmetry Approaches. Chem Phys Lett. 2000; 319:223–230.
17. Yamaguchi, K.; Takahara, Y.; Fueno, T. Applied Quantum Chemistry. Smith, VH.; Schaeffer, HF., III; Morokuma, K., editors. Reidel; Dordrecht: 1986. p. 155
18. Löwdin PO. Quantum Theory of Many-Particle Systems. 1. Physical Interpretations by Means of Density Matrices, Natural Spin-Orbitals, and Convergence Problems in the Method of Configurational Interaction. Phy Rev. 1955; 97:1474–1489.

19. Wang J, Becke AD, Smith VH Jr. Evaluation of [S-2] in Restricted, Unrestricted Hartree-Fock, and Density-Functional Based Theories. J Chem Phys. 1995; 102:3477–3480.
20. Sinnecker S, Neese F, Lubitz W. Dimanganese Catalase-Spectroscopic Parameters from Broken-Symmetry Density Functional Theory of the Superoxidized Mn-III/Mn-IV State. J Biol Org Chem. 2005; 10:231–238.
21. Onitsuka S, Aoki Y. Guidelines Proposed for Designing Organic Ferromagnets by Using a Quantum Chemical Approach. Theor Chem Acc. 2011; 130:789–806.
22. Rong C, Lian S, Yin D, Zhong A, Zhang R, Liu S. Effective Simulation of Biological Systems: Choice of Density Functional and Basis Set for Heme-Containing Complexes. Chem Phys Lett. 2007; 434:149–154.
23. Zhang L, Crossley MJ, Dixon NE, Ellis PJ, Fisher ML, King GF, Lilley PE, MacLachlan DR, Pace J, Freeman HC. Spectroscopic Identification of a Dinuclear Metal Centre in Manganese(II)-Activated Aminopeptidase P from Escherichia coli: Implications for Human Prolidase. J Biol Inorg Chem. 1998; 3:470–483.
24. Anderson PW. Antiferromagnetism. Theory of Superexchange Interaction. Phys Rev. 1950; 79:350–356.
25. Yu SB, Lippard SJ, Shweky I, Bino A. Dinuclear Manganese(II) Complexes with Water and Carboxylate Bridges. Inorg Chem. 1992; 31:3502–3504.
26. Khangulov SV, Pessiki PJ, Barynin VV, Ash DE, Dismuskes GC. Determination of the Metal-Ion Separation and Energies of the 3 Lowest Electronic States of Dimanganese(II,II) Complexes and Enzymes - Catalase and Liver Arginase. Biochemistry. 1995; 34:2015–2025. [PubMed: 7849059]
27. Liu SB, Perera L, Pedersen LG. Binuclear Manganese(II) Complexes in Biological Systems. Mol Phys. 2007; 105:2893–2898.

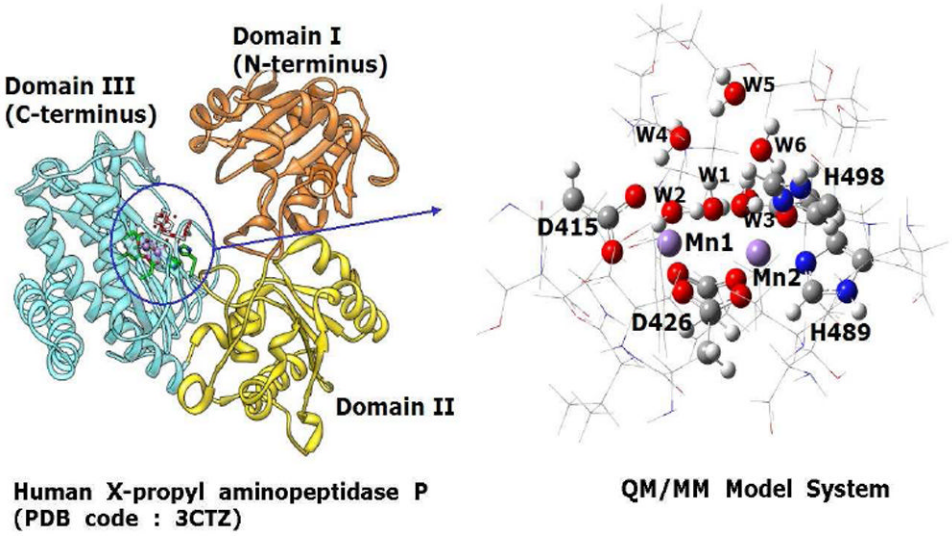

Figure 1.

A QM/MM model system for human cytosolic X-propyl aminopeptidase P. QM is shown in a ball-stick representation and the MM region is shown as a line. Carbon atoms are shown in gray, nitrogen atoms in blue, oxygen atoms in red, and hydrogens atoms in white. Two manganese atoms (Mn1 and Mn2) are shown in violet.

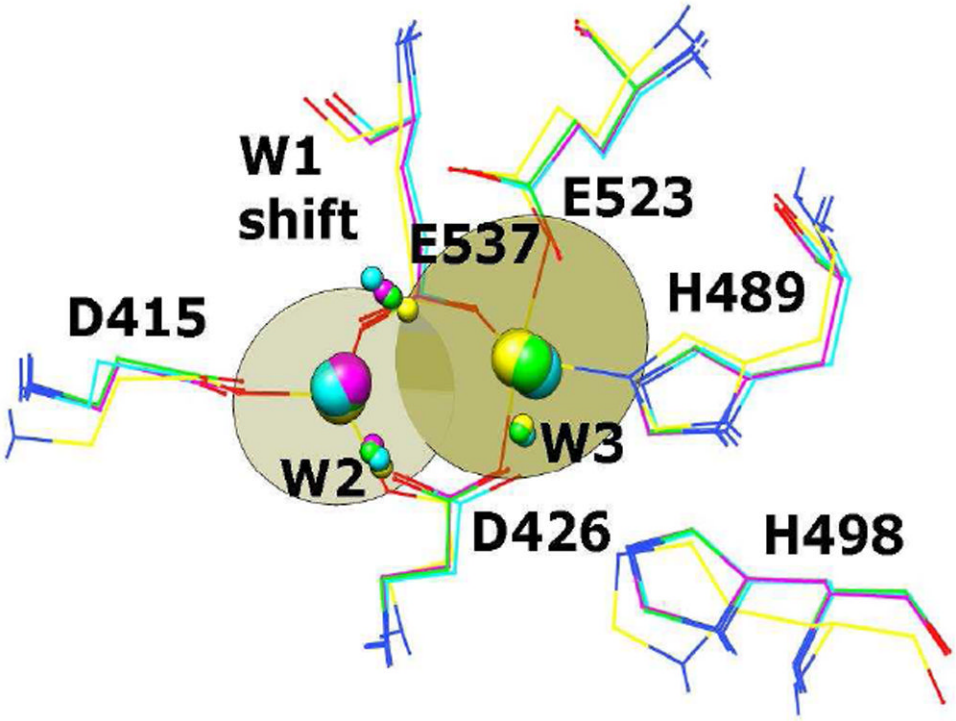

Figure 2.

Geometrically optimized structures for the different metal ions substituted at the site 1 (Top view). The only oxygen of water molecules W1, W2 and W3 are shown: Ca(II) (Cyan), Mg(II) (Magenta), Fe(II) (Green) and Mn (II) (Cyan). Side chains (represented as wire) and metal ions: Ca(II) (Cyan), Mg(II) (Magenta), Fe(II) (Green) and Mn (II) (Yellow). The two imaginary planes are shown; one for trigonal bypyramid geometry (site 1) and the other one for octahedron geometry (site 2). For clarity, some of the residues in MM region are not shown. Three water molecules (W1) are located on the same plane, but the positions of W1 are not conserved according to the metal ions substitution at the site 1. The plane at the site 1 is composed of Oδ-1 (D415), W1, and Oδ-1 (D426). On the other hand, the plane at the site 2 is composed of Oδ-2 (D426), Oε-2 (E523), Nε-2 (H489), and W1.

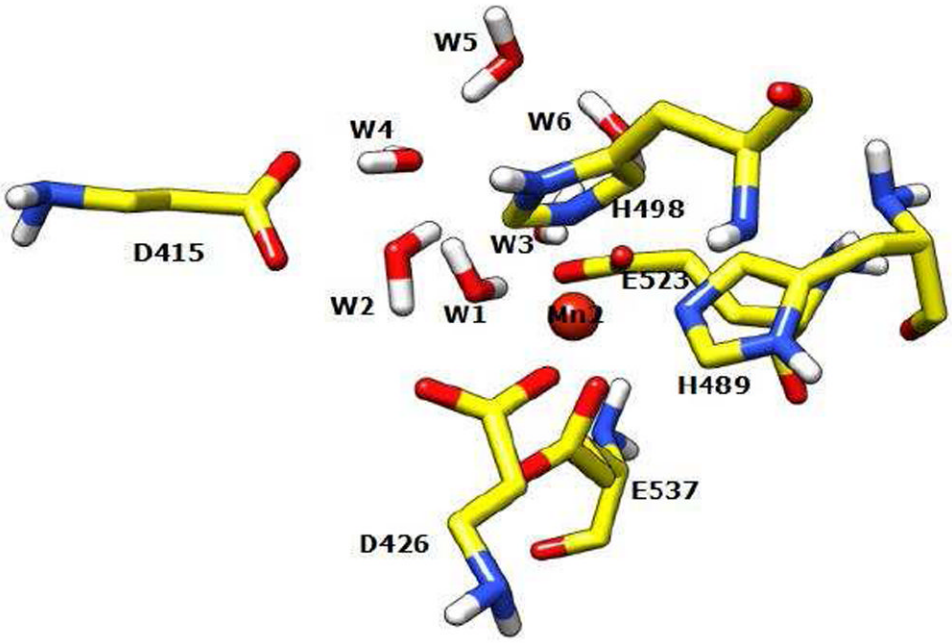

Figure 3.
Geometrically optimized structure for single manganese atom in the structural position with the vacancy of metal ion at the site 1. For clarity, some of the residues in the MM region are not shown.

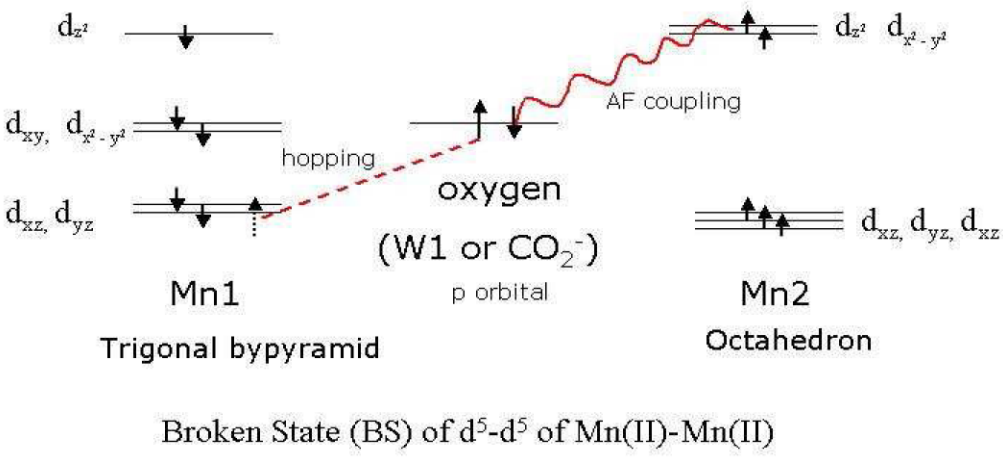

Figure 4.

A schematic atomic orbitals participating in the antiferromagnetic superexchange interaction between the two manganese atoms. The energy splitting of the local atomic orbitals of the Mn(II)-Mn(II) according to the crystal field environment are schematically illustrated. Relative energy splitting is arbitrary. One of the electrons from p orbitals provided by (W1 or CO_2^-) (d_{yz}, for instance) to make doubly occupied virtual state ("superexchange"). The unpaired electron at the p orbital couples to the electron of the one of five d orbitals (d_z^2) at Mn2. The two electrons localized at the manganese atoms are coupled by superexchange antiferromagnetically [11].

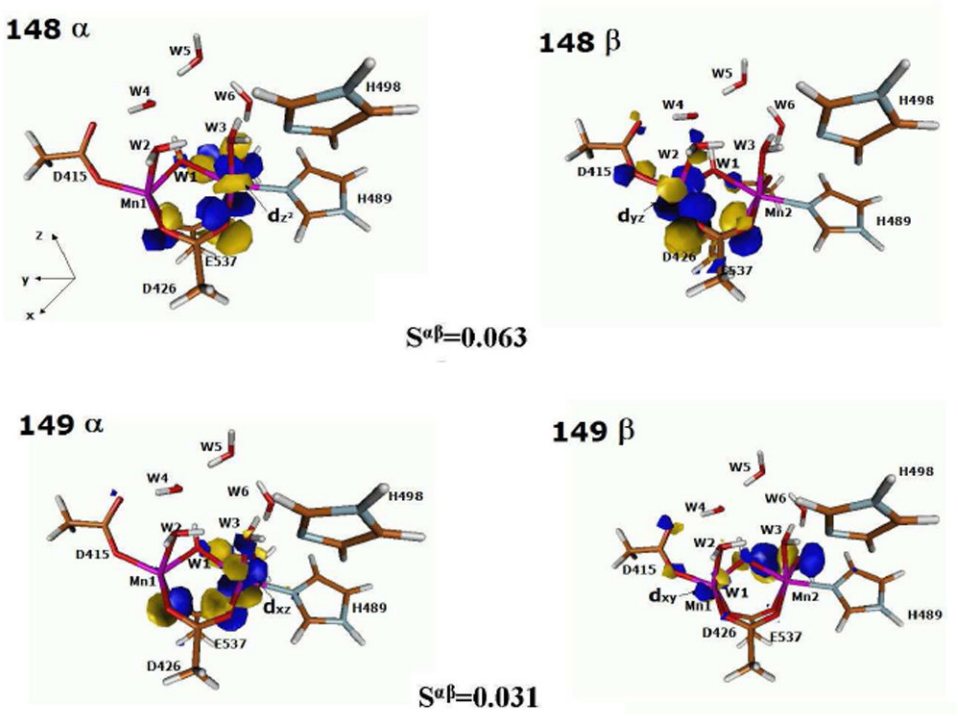

Figure 5.

Two dominant antiferromagnetic superexchange pathways. $S^{\alpha\beta}$ is defined as the overlap between two magnetic MO at the center of dinuclear manganese atoms. After the optimization, we performed QM single point calculation with all the MM region excluded at ORCA package to obtain broken symmetry solution.

Table 1

Coordination of the Mn(II)-Mn(II) Atoms at the Active Site. Unit Å

	Mn1					Mn2						
	D415 *Oδ*-1	**D426 *Oδ*-1**	**E537 *Oε*-1**	**W1**	**W2**	**D426 *Oδ*-2**	**E523 *Oε*-2**	**E537 *Oε*-2**	**H489 *Nε*-2**	**W1**	**W3**	**distance**
X-ray	2.15	2.14	2.19	2.23	2.27	2.37	2.27	2.26	2.27	2.31	2.17	3.42
Mn-Mn(S=5)	2.02	2.11	2.12	2.17	2.36	2.19	2.22	2.09	2.22	2.50	2.24	3.47
Ca-Mn(S=1/2)	2.22	2.29	2.31	2.28	2.46	2.04	2.04	1.99	2.13	3.71	2.13	3.74
Ca-Mn(S=5/2)	2.22	2.29	2.33	2.30	2.41	2.17	2.14	2.05	2.22	3.80	2.24	3.86
Fe-Mn(S=1/2)	2.11	1.99	1.97	2.00	2.10	2.04	2.00	1.97	2.17	3.68	2.00	3.44
Fe-Mn(S=9/2)	1.96	2.05	2.10	2.08	2.31	2.17	2.15	2.05	2.22	3.13	2.22	3.58
Mg-Mn(S=1/2)	1.94	2.01	2.04	2.06	2.23	2.12	2.09	2.01	2.06	2.23	2.10	3.19
Mg-Mn(S=5/2)	1.97	2.03	2.05	2.04	2.19	2.16	2.15	2.05	2.05	3.21	2.23	3.55
Mg-Mg(S=0)	1.96	2.04	2.05	2.04	2.20	2.07	2.07	1.98	2.16	3.33	2.10	3.59
vac-Mn(S=5/2)						1.91	2.01	1.88	2.34	2.25	2.01	

Table 2

EPR Experimental Data for Dinuclear Manganese, Mn(II)-Mn(II), Cluster with (μ-H_2O) and bis(μ-carboxylato) and Dimanganese Enzymes

	J(cm^{-1})	distance[a] (Å)
$[Mn_2(H_2O)(piv)_2(Me_2bpy)_2]$[b]	-2.73	3.595
$[Mn_2(H_2O)(CH_3CO_2)_4(L)_2]$[c]	-2.952	3.621
dimanganese catalyze[d]	-5.6±0.1	3.59
arginase[e]	-2.0±0.5	3.50

[a] Mn(II)-Mn(II) distance

[b] piv: pivalate, Me2bpy: 4,4'-dimethyl-2,2'-bipyridine[25].

[c] L:N,N,N',N'-tetramethylethylenediamine [25].

[d] Phosphate derivative of dimanganese catalyse from *Thermus thermophilus*[26].

[e] Arginase from rat liver with addition of borate[26].